



Light assisted solar fuel production by artificial CO₂ Reduction and water Oxidation

Deliverable D5.1

Photocathode/OPV/dark anode half-cell

| | |
|----------------------|------------|
| Lead Beneficiary: | EPFL |
| Delivery date: | 31/08/2023 |
| Dissemination level: | Public |
| Version: | v1.0 |



This Project has received funding from the European Union's Horizon 2020 research and innovation programme under grant agreement No. 951843

D5.1 Photocathode/OPV/dark anode half-cell

Document Information

| | |
|----------------------------------|---------------------------------------|
| Grant Agreement Number | 951843 |
| Acronym | LICROX |
| Start date of project (Duration) | 01/09/2020 (36 months) |
| Document due date | 31/08/2023 |
| Submission date | 31/08/2023 |
| Authors | Ian Sharp |
| Deliverable number | D5.1 |
| Deliverable name | Photocathode/OPV/dark anode half-cell |
| WP | WP5 – PEC implementation & validation |

| Version | Date | Author | Description |
|---------|------------|---------------------|---|
| v 0.1 | 20/08/2023 | Anna Loudice (EPFL) | Creation first draft |
| v 0.2 | 30/08/2023 | Ian Sharp (TUM) | Revision |
| v 1.0 | 31/08/2023 | Laura López (ICIQ) | Final version after revision and approval by the Management Board |

EXECUTIVE SUMMARY

This document, is a public report that contains information about the final photocathode/catalyst structure developed in LICROX. Given the confidential nature of the work, the detailed conditions are discussed in general terms. The basic properties of the photocathode/catalyst structure and their representative performance characteristics are described. D5.1 Photocathode/OPV/dark anode half-cell, is a deliverable of the LICROX Project, which is funded by the European Union's H2020 Programme under Grant Agreement No. 951843. Due to the instability of the photocathode at potentials where copper catalysts generate C2 products targeted within the project, fabrication and test performance of the PEC with the configuration photocathode/OPV/dark anode was not achieved and will not be discussed.

D5.1 Photocathode/OPV/dark anode half-cell

Table of Contents

| | |
|--|---|
| WP5. PEC implementation & validation | 4 |
| 1. Description of the photocathode structure | 4 |
| 2. Assembly photocathode/catalyst | 5 |
| 3. Electrochemical testing and performance of the assembly | 6 |
| 4. Conclusions | 7 |
| 5. References | 7 |

D5.1 Photocathode/OPV/dark anode half-cell

WP5. PEC implementation & validation

In WP5 the catalysts, semiconductors and light trapping strategies developed in WPs 2, 3 & 4, respectively, will be assembled together to build and test the performance of different PEC configurations. The implementation of the activities in this WP targets:

- i) Assembly of the materials and optimal light trapping configurations into one single device by multi-layering or by stacking and connection through conductive materials;
- ii) Assessment of the current output of the device upon simulated sun illumination; and
- iii) Quantification of the chemical products obtained from the current output and determination of Faradaic efficiencies and solar to chemical energy efficiency.

1. Description of the photocathode structure

Within LICROX, initial efforts on the photocathode were addressed to the synthesis of CuFeO_2 thin films, however due to instability problems, the research was re-focused to the use of Cu_2O . The research work carried out within the frame of the project allowed to reach interesting results in the use of this material based on a protection strategy to improve stability, however not optimal conditions have been achieved yet to run the envisaged tests with the OPV attachment structure, therefore only advances on the use of the photocathode/catalyst structure are reported herein.

The protected Cu_2O photocathode was synthesized by a combination of electrochemical deposition and ALD methods. The overall steps to build the developed structure are depicted in Figure 1a. The cross-sectional scanning electron microscopy image (Figure 1b), shows a planar Cu_2O film with a homogeneous thickness electrochemically deposited on FTO coated with Au, as previously reported.¹ The selected ALD protection layer consists of a Ga_2O_3 ALD layer of 10 nm thickness followed by the ALD deposition of a 20 nm TiO_2 layer produced following a recently reported procedure.² Ga_2O_3 was preferred to the more traditional Al doped ZnO layer because of the demonstrated shift of the onset potential at more positive potentials due to a better band alignment of the Ga_2O_3 with Cu_2O that reduces interfacial recombination, increasing the photovoltage.² In order to increase the catalyst loading, ensure high interfacial contact area, and avoid aggregation, we deposited a porous layer on top of the protected photocathode. A transparent TiO_2 porous layer is ideal for this purpose. Specifically, colloidal anatase TiO_2 nanorods (NRs) with a size of $20 \times 3 \text{ nm}^2$ were synthesized via a reported colloidal synthesis. The obtained TiO_2 NRs come as a colloiddally stable ink in organic solvents (such as hexane and toluene) thanks to their native ligands. A representative transmission electron microscopy (TEM) image of the TiO_2 NRs is reported in Figure 1c. This ink can be easily spin coated on top of the protect Cu_2O to obtain a porous film of 100 nm thickness. The native organic ligands are subsequently removed via O_2 plasma to avoid problems in charge transfer due to the insulating nature of the ligands and to allow

D5.1 Photocathode/OPV/dark anode half-cell

the deposition of a second layer. By repeating these steps multiple times, a porous layer of around 600 nm thickness can be obtained and is shown in the SEM image in Figure 1b.

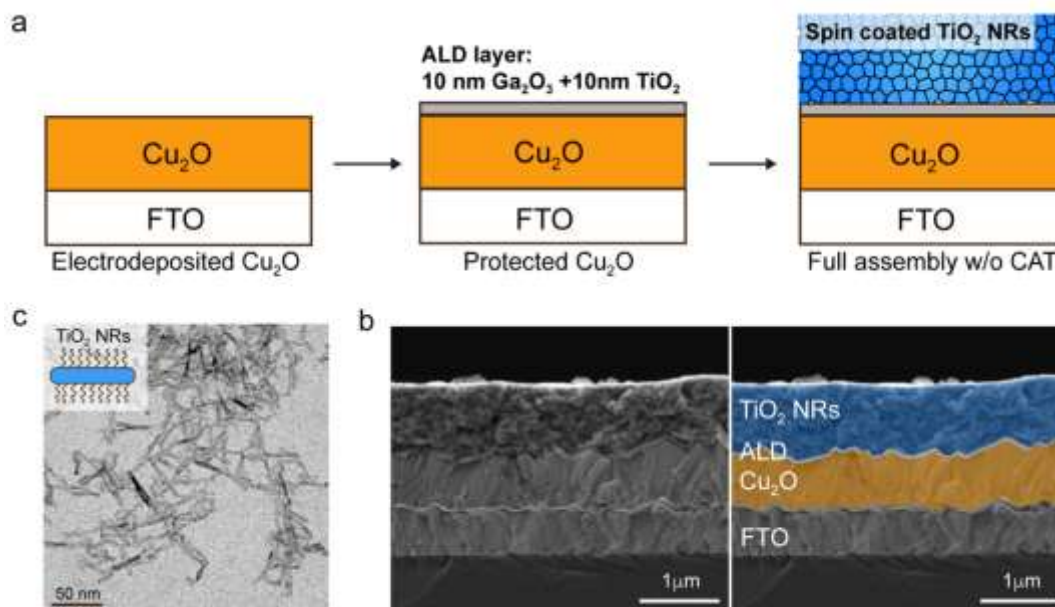


Figure 1. a) Schematic of the process used to fabricate the photocathode structure used in this work; b) SEM cross-section image of the photocathode without catalyst; c) TEM image of the anatase TiO₂ NRs used to build the porous layer.

2. Assembly photocathode/catalyst

Different catalysts active for electrochemical CO₂RR were integrated with the above-described photocathode. Specifically, we have selected three catalysts based on the one developed within the LICROX project: copper cubes of 44 nm edge (Cu_{Cub}), gold spheres of 8 nm size (Au_{Sph}) and iron porphyrin modified with a COOH group (FePyCOOH). The corresponding TEM images and the chemical structures are shown in Figure 2a. Cu_{Cub} and Au_{Sph} were integrated into the structure by a simply drop-casting 60ugr of a dilute catalyst solution on the porous layer. FePyCOOH instead is bounded to the surface of the porous layer upon overnight immersion of the electrode in a 1mM solution of the catalyst.

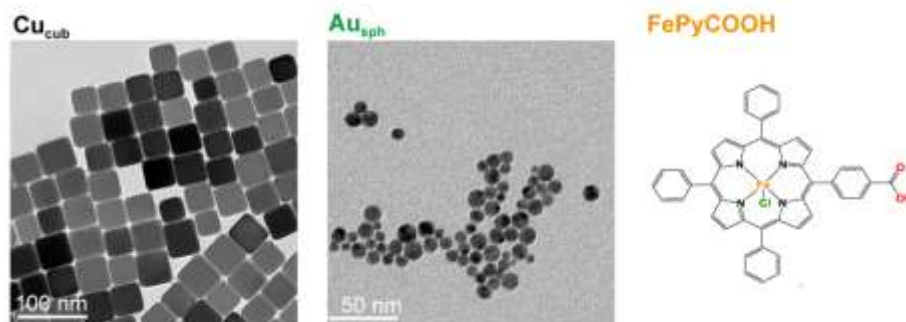


Figure 2. TEM images and chemical structure of the tested catalysts.

D5.1 Photocathode/OPV/dark anode half-cell

Cu_{cub} are well known to be able to electrochemically reduce CO_2 to multi-carbons products with high selectivity for ethylene, while Au_{sph} and FePyCOOH have been reported to be highly selective for CO. Nevertheless, such catalysts have not been previously tested for PEC CO_2RR , especially using Cu_2O as a photocathode in aqueous electrolyte.

One stark difference among those catalysts is that when tested in dark under the same conditions of 0.1M KHCO_3 electrolyte in a two-compartment cell separated by a proton exchange membrane, those catalysts are active for CO_2RR in different potential ranges. Specifically, Cu_{cub} can generate multicarbon products in dark conditions, but only at potentials more negative than -0.9V vs RHE, while Au_{sph} can reduce CO_2 to CO at potentials more negative than -0.4V vs RHE and FePyCOOH at potentials more negative than -0.6V vs RHE.

3. Electrochemical testing and performance of the assembly

Following assembly of the complete photocathode/protection layer/support/catalyst structure, we tested the three catalysts under 1 Sun illumination at constant applied potential in 0.1M KHCO_3 . We observed that for potentials more negative than 0V vs RHE, the full assembly is unstable due to degradation of the protection layer. Therefore, we have limited our study to an applied potential of 0V vs RHE and we have collected the generated products over time. We note that the photocathode structure was not tested together with the OPV, since the photovoltaic element would drive the photocathode outside of its stability window.

Under illumination of 1 Sun illumination in 0.1M KHCO_3 electrolyte, we could measure a generated photovoltage of around 450 mV. Considering the above-described potential dependence of the product distribution for each of the selected catalysts, we expect that only Au_{sph} could perform CO_2RR over HER when a bias of 0V vs RHE is applied. Indeed, in Figure 2, we can observe that Au_{sph} can reduce CO_2 to CO with a FE of 50% with a photocurrent of approximately $-0.7\text{mA}/\text{cm}^2$. This result demonstrates that PEC CO_2RR is possible with the developed assembly. From the other side, Cu_{cub} and FePyCOOH can produce mostly H_2 (data not shown).

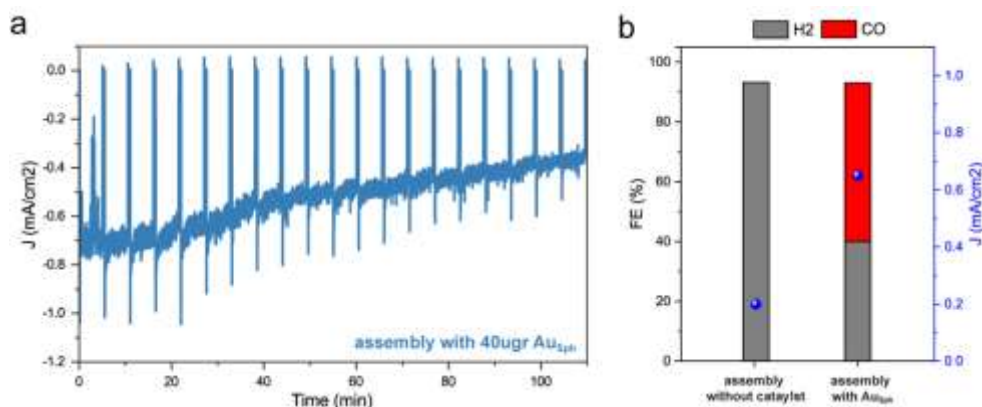


Figure 3. a) Chronoamperometric measurements of the full assembly FTO/ Cu_2O /ALD/ TiO_2 NRs/ Au_{sph} in 0.1M KHCO_3 at 0V vs RHE. b) Product distribution for the assembly with and without catalyst under 1 Sun illumination at 0V vs RHE in 0.1M KHCO_3 .

D5.1 Photocathode/OPV/dark anode half-cell

4. Conclusions

A photocathode assembly based on Cu_2O light absorber and able to generate a reasonably stable photocurrent of $-0.7\text{mA}/\text{cm}^2$ at 0V vs RHE in aqueous electrolyte has been developed. When Au_{sph} catalyst is integrated, syngas can be generated with a FE of 50%. To the best of our knowledge this is the first time that syngas can be generated in aqueous electrolyte under 0V bias using photoelectrochemical renewable energy source generated by an earth abundant photocathode. In order to move towards multi-carbon product generation, a novel strategy to protect the Cu_2O must be developed or new catalysts able to reduce CO_2 at more positive potentials needs to be discovered.

5. References

- 1) A. Paracchino, V. Laporte, K. Sivula, M. Grätzel, E. Thimsen. *Nature Materials*, 10, 456–461 (2011).
- 2) L. Pan, J. H. Kim, M. T. Mayer, M.-K. Son, A. Ummadisingu, J. Sung Lee, A. Hagfeldt, J. Luo, M. Grätzel. *Nature Catalysis*, 1, 412–420 (2018).